Title: Forest structural diversity is linked to soil microbial diversity

Ashley K. Lang*[1], Elizabeth A. LaRue[2], Stephanie N. Kivlin[3], Joseph D. Edwards[3], Richard P. Phillips[1], Joey Gallion[4], Nicole Kong[5], John D. Parker[6], Melissa K. McCormick[6], Grant Domke[7], Songlin Fei[8]

Affiliations:

[1]Department of Biology, Indiana University, Bloomington, IN, USA

[2]Department of Biological Sciences, The University of Texas at El Paso, El Paso, TX, USA

[3] Department of Ecology and Evolutionary Biology, University of Tennessee, Knoxville, Knoxville, TN, USA 37996

[4]Indiana Department of Natural Resources, Indianapolis, IN, USA

[5]Purdue University Libraries, Purdue University, West Lafayette, IN, USA

[6]Smithsonian Environmental Research Center, MD, USA

[7]U.S. Department of Agriculture, Forest Service, Northern Research Station, St. Paul, MN, USA

[8]Department of Forestry and Natural Resources, Purdue University, West Lafayette, IN, USA

*Corresponding author: al40@iu.edu

Summary

1) In addition to taxonomic diversity, the structural diversity of plant communities may be related to the diversity of soil bacterial and fungal communities, which fuel important ecosystem processes but are difficult to characterize across broad spatial scales. We investigated the potential for using remotely sensed information (e.g. using Light Detection and Ranging - LiDAR) about forest structural diversity as a predictor of soil microbial community composition.

2) We calculated LiDAR-derived metrics of structural diversity as well as a suite of stand and soil properties from hardwood forests across Indiana, USA to test whether forest canopy structure is linked with the community richness and diversity of four key soil microbial groups: bacteria, fungi, arbuscular mycorrhizal (AM) fungi, and ectomycorrhizal (EM) fungi.

3) We found that the density of canopy vegetation is positively associated with the taxonomic richness of EM fungi, and that structural diversity metrics are associated with the overall community composition of bacteria, EM, and total fungal communities.

4) Remotely sensed metrics of forest structural diversity may be used to estimate the richness and community composition of soil microbial groups. Establishing links between structural and microbial diversity could facilitate the detection of belowground biodiversity hotspots.

Keywords: Forest structure, LiDAR, microbial biogeography, plant-fungal associations, soil biodiversity

Introduction

Explaining the causes of biodiversity is at the forefront of ecological inquiry because many facets of diversity contribute to ecosystem function (Loreau *et al.*, 2001). First principles suggest that diversity begets diversity, and that diversity at one trophic level should be positively associated with diversity at another trophic level. However, it is less clear if this pattern applies to plants and their associated soil microbial communities (Fei *et al.*, 2022). While above ground plant diversity has been well characterized, cataloging belowground diversity and its linkages with above ground diversity at broad spatial scales has been more difficult. This is especially true for soil microbial diversity, where soil samples must be collected, sequenced and analyzed before information about diversity can be obtained. Furthermore, much of the research linking above- and belowground diversity in forests has been based on tree species richness (e.g. Vogelsang et al. 2006, Li et al. 2020), but previous work has shown that the direction and strength of these relationships between tree species richness and microbial diversity, including that of mycorrhizal fungi, vary (Wagg *et al.*, 2015; Fei *et al.*, 2022).

The three-dimensional (3D) volume and arrangement of vegetation within the ecosystem (structural diversity) is an overlooked aspect of ecological diversity (LaRue et al. In Revision) that may also be linked to microbial diversity. Structural diversity can be easily estimated with remote sensing (Zeng *et al.*, 2022) and provides an opportunity to capture multiple aspects of biodiversity (D'Urban Jackson *et al.*, 2020; Valbuena *et al.*, 2020). Structural diversity represents functional variation in plant size that creates habitat and supports ecosystem functions that are linked to the biodiversity of soil organisms (Taboada *et al.*, 2010). Of particular interest are potential linkages between the structural diversity of vegetation and the diversity of soil

microbial communities, because together these organisms control ecosystem productivity and biogeochemical cycling (Zak *et al.*, 2003; Wagg *et al.*, 2011, 2019). Yet, it is still unclear whether the structural diversity of plant communities is related to the diversity of soil bacteria and fungi, and whether these remotely-sensed metrics of aboveground structural diversity may be used to predict soil microbial diversity and belowground ecosystem processes.

There are several ways in which forest structural diversity may affect soil microbial diversity. First, above ground structural diversity should be positively linked to below ground structural diversity. More structural complexity belowground may result from a wider variety of root morphologies, including branching architecture and rooting depths, that provide microbial habitats and thus a more diverse microbial community (McCormack *et al.*, 2015). Second, structural diversity is known to be positively associated with higher light capture and complementary resource use by trees, which supports higher forest productivity (Ishii *et al.*, 2004; Gough *et al.*, 2019). Structural diversity may therefore enhance ecosystem productivity and carbon fixation that fuels both the soil decomposer and mycorrhizal fungal communities (Anthony *et al.*, 2022). Third, above- and below-ground structural diversity change as trees age (Matsuo *et al.*, 2021), and root-associated microbial taxa will shift with tree age and nutrient demand (Gange *et al.*, 1993; Johnson *et al.*, 2005). Through these pathways, changes in structural diversity of forest canopies may have cascading impacts on the composition of soil bacterial and fungal communities.

Microbial guilds, including mycorrhizal fungal guilds, may differ in their relationships with structural diversity. For example, decomposers may respond positively to increasing canopy complexity owing to higher productivity of forests that are structurally diverse above ground and can capture more light resources (Gough *et al.*, 2019). As a result, these forests may support larger pools of coarse woody debris and faster root turnover with higher rates of tree growth, supplying decomposers with more substrate than forests with less complex canopies. Patterns in the community structure of mycorrhizal fungi, however, are more likely to follow from tree species traits, including root morphology, tree species richness, and forest age structure, as different mycorrhizal functional guilds tend to associate with certain tree species, and mycorrhizal communities tend to differ with tree age class (Brundrett, 2004; Johnson *et al.*, 2005; Aučina *et al.*, 2011; Ferlian *et al.*, 2021). However, mycorrhizal fungal diversity may be influenced by structural diversity via the effects of forest age structure: uneven-aged stands are

likely to have higher structural diversity and a wider variety of host tree ages to support more distinct mycorrhizal taxa. Further, more productive host trees tend to supply mycorrhizal fungi with larger quantities of carbon, so faster-growing, structurally complex forests may also harbor distinct communities of mycorrhizal fungi with higher carbon demand compared with slower-growing stands (Anthony *et al.*, 2022). Therefore, bacterial and fungal decomposers may be influenced most by the variety of substrates available in highly structurally diverse forests, whereas mycorrhizal fungi may be linked with variation in tree age, productivity, and physiology (Comas *et al.*, 2014; Birch *et al.*, 2021; Anthony *et al.*, 2022).

To identify potential linkages between above- and belowground diversity, we tested for correlations between structural and soil microbial diversity across the central hardwood region, USA (Figure 2). We expected that structural diversity would be a significant predictor of soil bacterial and fungal, including mycorrhizal fungal, richness (alpha diversity) and community composition (beta diversity). We also predicted that connections between plant structural diversity and soil microbial diversity would be equally strong or stronger than relationships between plant and microbial diversity. We also examined the relative predictive ability of tree species richness (Wu *et al.*, 2019), stand age and productivity (Högberg *et al.*, 2007; Wagg *et al.*, 2011), climate (Pold & DeAngelis, 2013; Nottingham *et al.*, 2018), and soil properties to explain variation in soil microbial richness and community composition. In particular, we included several soil factors with known effects on microbial community composition, including pH (Rousk *et al.*, 2009; Davison *et al.*, 2021) , carbon to nitrogen ratio (Midgley & Phillips, 2016; Soares & Rousk, 2019), and mineral composition (represented by oxalate-extractable iron content; (Carson *et al.*, 2009; Whitman *et al.*, 2018)). Remote sensing technologies that can resolve 3D structural diversity (e.g. Light Detection and Ranging - LiDAR) are becoming readily available from landscape to global scales. Identifying linkages between above-and belowground diversity will provide the potential to map indicators of belowground diversity across large spatial scales, which could become an important tool for managing ecosystem functions and soil biodiversity that might otherwise be difficult to monitor without time consuming genomic and chemical analyses of soils.

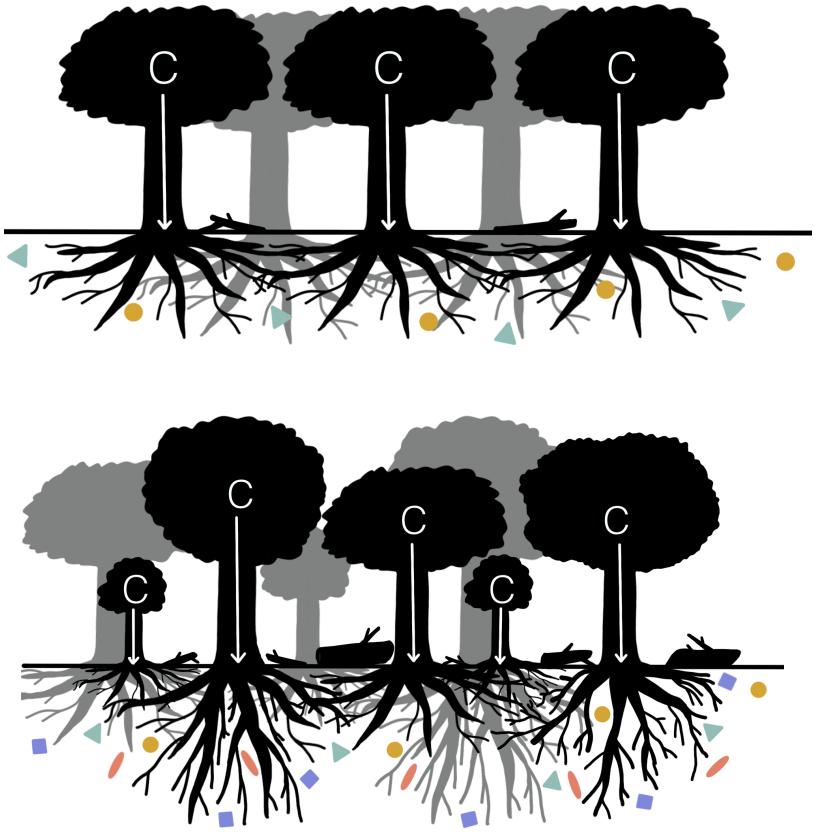

Figure 1. Forest structural diversity may influence soil microbial diversity through several pathways. A less structurally diverse forest (A) may support lower soil microbial diversity due to lower productivity and belowground carbon allocation, less coarse woody debris, and less complex rooting architecture relative to that of a more structurally diverse stand (B). Shapes indicate different microbial taxa.

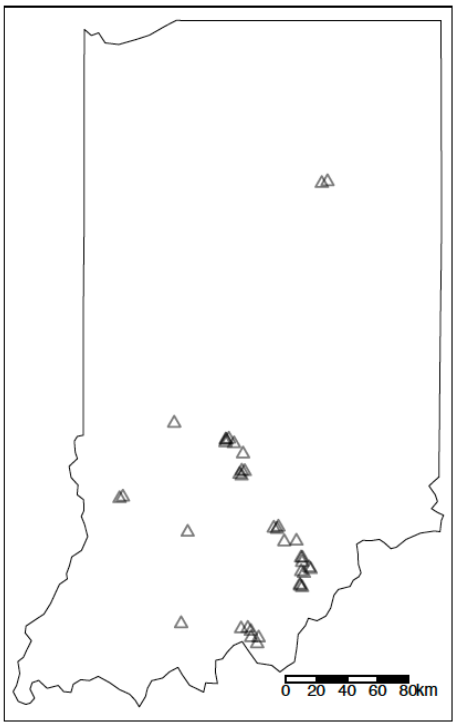

Figure 2. Location of study sites within the central hardwood region of Indiana, USA (N_{Plots} = 38).

Materials and methods

Forest structural diversity and stand properties

We obtained inventory data on 38 forest plots from the Indiana Continuous Forest Inventory (CFI) (Gallion, 2018; Figure 2). Individual trees (minimum diameter 12.7 cm) are identified to species and have their dbh measured every five years. We estimated tree species richness and productivity with the individual tree-level data from the growing season of 2020 (May to October). Total tree species were calculated as the number of unique tree species found within each 7.3 m radius circular plot. The change in basal area of trees over the five year interval was used as a predictor of plot productivity, which was calculated as the annual increase in basal area from from 2015 to 2020. Stand age was obtained for each plot from the CFI database. Finally, the type of mycorrhizal association for each tree host was classified following (Jo *et al.*, 2018) and used to calculate ectomycorrhizal (EM) and arbuscular mycorrhizal (AM) host richness and abundance (basal area m^{-2}). The dominance of AM trees was calculated by dividing the AM tree basal area by the sum of AM and EM tree basal area (Jo *et al.*, 2018).

To quantify the above-ground structural diversity of forests, we obtained discrete return LiDAR from the 2017-2019 USDA 3DEP survey (USGS, 2020). Details about the collection and specifications of the 3DEP LiDAR can be found on the USDA 3DEP website (https://www.usgs.gov/3d-elevation-program). A 30 m radius buffer area was clipped around the plot centroid. Large groups of atmospheric and ground outliers were filtered by removing points above and below six standard deviations of the mean height and then manually checked to ensure that outliers were actually removed. All LiDAR processing was conducted in the *lidR* (v. 3.1.2)

R package (Roussel *et al.*, 2020; Roussel & Auty, 2022). The buffer area was then corrected for elevation using a Delaunay triangulation before being clipped to a 7.3 ft radius circular plot. Three structural diversity metrics were calculated from each plot area that represent the volume and arrangement of structural diversity in forests (LaRue *et al.*, 2020). These metrics were chosen based on stability across different LiDAR point densities (i.e. 2-8 points per m^2) (LaRue *et al.*, 2022). Points below 0.5 m were filtered from the point cloud to exclude ground points and the following metrics were calculated: the standard deviation of the height of points, vegetation area index, and vertical complexity index. Vegetation area index (VAI) describes the density of vegetation within forest canopies and was calculated with the LAD function from the *lidR* package (Roussel *et al.*, 2020). The standard deviation of vegetation heights (VertSD) and vertical complexity index (VCI) describe the vertical heterogeneity of vegetation throughout the vertical canopy profile. VertSD was calculated from the cloud_metrics function and VCI from the VCI function in the *lidR* package.

Microbial diversity and soil chemistry

Two soil cores (~200 cm^3) were collected on the perimeter of each plot in 2020 during the growing season; one core was collected each from the east and west sides of the plot. The cores were subdivided into two depths (0-5 cm and 5-10 cm) and homogenized within depths at the time of collection. Samples were air dried and passed through a 2 mm sieve prior to chemical and microbial analyses. The percent soil carbon and nitrogen content were determined using an elemental combustion system (Costech ECS 4010, Costech Analytical Technologies, Valencia, CA, USA). Iron, which is a proxy for mineral soil reactivity, was extracted from a 200 mg subsample of soil from each plot and each depth with an oxalate solution. Oxalate-extractable iron concentration was determined on a mass percent basis using atomic absorption spectrometry (PerkinElmer Instruments, Waltham, MA, USA).

DNA was extracted from ~ 250 mg of homogenized soil from 0-5 and 5-10 cm core depths of each plot using the Qiagen DNeasy Soil Extraction kit (Qiagen, Germantown, MD, USA). DNA was quantified with the Qubit high sensitivity kit (Qubit Fluorometer, Life Technologies, Carlsbad, CA, USA) and diluted to ~10 ng/µl in sterile water. We amplified fungi using barcoded 5.8-Fun and ITS4-Fun primers targeting the ITS2 region (Taylor *et al.*, 2016), and bacteria via barcoded S-D-Bact-0341-b-S-17 and S-D-Bact-0785-a-A-21 primers of the 16S region (Klindworth *et al.*, 2013). Each PCR contained 5 µL of ~1-10 ng/µL DNA template, 21.5

194 µL of Platinum PCR SuperMix (Thermo Fisher Scientific Inc., Waltham, MA), 1.25 µL of each
195 primer (10 µM), 1.25 µL of 20 mg/mL BSA, and 0.44 µL of 25 mM MgCl2. For the ITS2
196 primers, the reactions included an initial denaturing step at 96 °C for 2 min, followed by 24
197 cycles of 94 °C for 30 sec, 51 °C for 40 sec, and 72 °C for 2 min, with a final extension at 72 °C
198 for 10 min. For the 16S primers, reactions started with an initial denaturing step at 95 °C for 5
199 min, followed by 25 cycles of 95 °C for 40 sec, 55 °C for 2 min, and 72 °C for 1 min, with a
200 final extension at 72 °C for 7 min. To accurately capture the AM fungal community, we
201 amplified AM fungal DNA separately. Due to limited AM fungal DNA, we first performed a
202 nested PCR reaction. The first reaction amplified a ~800b section of AM fungi and plants in the
203 18S region using the NS1 – NS4 primers (White *et al.*, 1990), the preferred marker gene for AM
204 fungi (Lekberg *et al.*, 2018). The nested reaction amplified a ~400b region of 18S AM fungal
205 DNA with barcoded Illumina TruSeq V3 indices (Illumina, San Diego, CA, USA) linked to the
206 NS31 -AML2 primers (Morgan and Egerton-Warburton 2017). Each reaction contained: 21.5 µl
207 of Platinum PCR Supermix (Invitrogen, Carlsbad, CA, USA), 1.25 µl of each primer (10 µM),
208 0.5 µl of BSA (20 mg/ml), and 2 µl (~20ng) of DNA. The first reaction ran at 94 °C for 3 min,
209 followed by 30 cycles of 94 °C for 30 sec, 40 °C for 1 min, and 72 °C for 1 min and the nested
210 reaction at 94 °C for 5 min, followed by 40 cycles of 94 °C for 45 sec, 63.1 °C for 1 min, and 72
211 °C for 1.5 min. In all cases, triplicate reactions were combined, cleaned with Agencourt AMPure
212 XP magnetic beads (Beckman Coulter, Brea, CA, USA), and quantitated fluorometrically (Qubit
213 Fluorometer, Life Technologies, Carlsbad CA, USA). Samples were pooled into equal amounts
214 and run on an Illumina MiSeq v3 sequencer in a 2 × 275 b run at the University of Tennessee
215 Center for Environmental Biotechnology core.

216 All sequences were processed in the DADA2 pipeline in R (Callahan *et al.*, 2016). First,
217 primers were trimmed from all sequences and sequence error rates were calculated. Sequences
218 were then merged into unique amplicon sequence variants (ASVs). Finally, chimeras were
219 removed using a denovo chimera checker. General fungal and bacterial sequences were matched
220 to taxonomy via the RDP and UNITE databases. Because the NS31-AML2 primers may amplify
221 some non-AM fungal fungi, we then BLASTed representative sequence reads from each ASV
222 against the MaarjAM database (Opik *et al.*, 2010) and only retained reads that matched a known
223 AM fungal virtual taxonomic unit by at least 97%. EM fungi were defined via the FungalTraits

database (Põlme *et al.*, 2020). Sequences are deposited in the NCBI Sequence Read Archive (Biosample to be provided upon publication).

We calculated alpha (taxonomic richness) and beta diversity (community composition) of bacteria, total fungi, EM and AM fungal groups. We calculated alpha diversity with the inverse Simpson's index using the *diversity* function in the *vegan* package in R (Oksanen *et al.*, 2022); although we tested several diversity metrics for this analysis, most metrics yielded qualitatively similar results, so we focus on inverse Simpson's index based on recommendations for mycorrhizal fungi (Morris *et al.*, 2014) and for simplicity of interpretation (*i.e.* larger values of Simpson's index indicate greater alpha diversity). We calculated beta diversity using the quantitative Jaccard index with the *vegdist* function in the *vegan* package (Oksanen *et al.*, 2022).

Statistical analyses

To test for relationships between variables related to above-ground vegetation and soil conditions and alpha diversity of the soil microbes, we constructed a suite of eight general linear regression models to test for significant relationships between microbial alpha diversity (species richness) and vegetation and soil conditions; separate models for alpha diversity were developed for each microbial guild (bacteria, all fungi, EM fungi, and AM fungi) at a given depth (0-5 and 5-10 cm). We calculated partial R^2 values using the *sensemakr* package in R (Cinelli *et al.*, 2021) and scaled model coefficients to allow for comparison of the strengths of model predictors (Gelman, 2008). Before developing the general linear regression models, we removed predictor variables that had a correlation coefficient greater than 0.70 (Fig. S1; Tabachnick & Fidell, 2013). Variable selection was based on relevance to our hypothesized drivers and designed to optimize the amount of information gained by keeping specific predictors in the model (Gregorich *et al.*, 2021). For example, AM and EM tree species richness were highly correlated with tree species richness (all trees) and AM dominance, so we removed AM and EM tree richness because total tree richness allowed us to preserve information about plant richness and AM dominance reflects the relative importance of both AM and EM tree species in each plot based on basal area. However, we also assessed correlations between microbial diversity and AM and EM host tree richness to ensure that patterns identified in our analyses were not due to underlying relationships between stand properties and host tree richness (Fig. S2). Finally, we evaluated our models with and without the random effect of county to account for spatial patterns in the locations of sampling plots. The effect of county was negligible in all models

(Table S1), and therefore we present the more parsimonious linear models without a random effect of county.

Next, we tested the significance and relative strength of structural diversity and other environmental variable categories for their ability to explain the variation in microbial community composition (i.e. community similarity among sites) at both 0-5 and 5-10 cm soil depths. We conducted a distance-based redundancy analysis using the dbrda function using the *vegan* package in R (Oksanen *et al.*, 2022) to assess patterns in the composition and structure of the total fungal community, the bacterial community, the AM fungi, and EM fungi. Factors contributing to the variation in beta-diversity were partitioned among four categories (Table 1) and we ran models with variables grouped into these categories and also separately to assess individual variable significance. For both variable groups and individual variables, we ran full full dbRDA models with all terms, then ran subsequent reduced models with only the terms with $p < 0.05$ from the full model. Variation in beta diversity due to spatial autocorrelation among plots was detrended prior to analysis. The explanatory power of each category indicated as significant by the dbRDA model was assessed using the varpart function in the *vegan* package. We used variance partitioning analysis to assess the relative importance of different drivers of site-to-site variation in overall community composition and structure, following recommended procedure for analyses of ecological beta diversity with community composition data (Legendre, 2008). Highly correlated variables within each category were removed before analysis (See Fig. S1: AM and EM tree richness, % N, % C).

Results

Structural diversity and environment linkages to microbial alpha diversity

Forest structural diversity was rarely associated with microbial richness, regardless of microbial guild, soil depth or forest structure metric (Table 2). The one exception was EM fungal richness in the upper surface soils, which was positively related to VAI (Table 2, Figure 3). Rather, microbial richness was mostly a function of edaphic factors. Soil pH had the strongest and most consistent effects on microbial richness in both the 0-5 and the 5-10 cm soil depth (Table 2). Alpha diversity of AM fungi, bacteria, and the total fungal community were positively associated with soil pH (Table 2, Figure S2). The total fungal community richness at 5-10 cm

depth was positively associated with basal area increment. Finally, older stands had greater EM fungal richness at 0-5 cm depth (Table 2), which was a stronger positive predictor of EM richness than VAI.

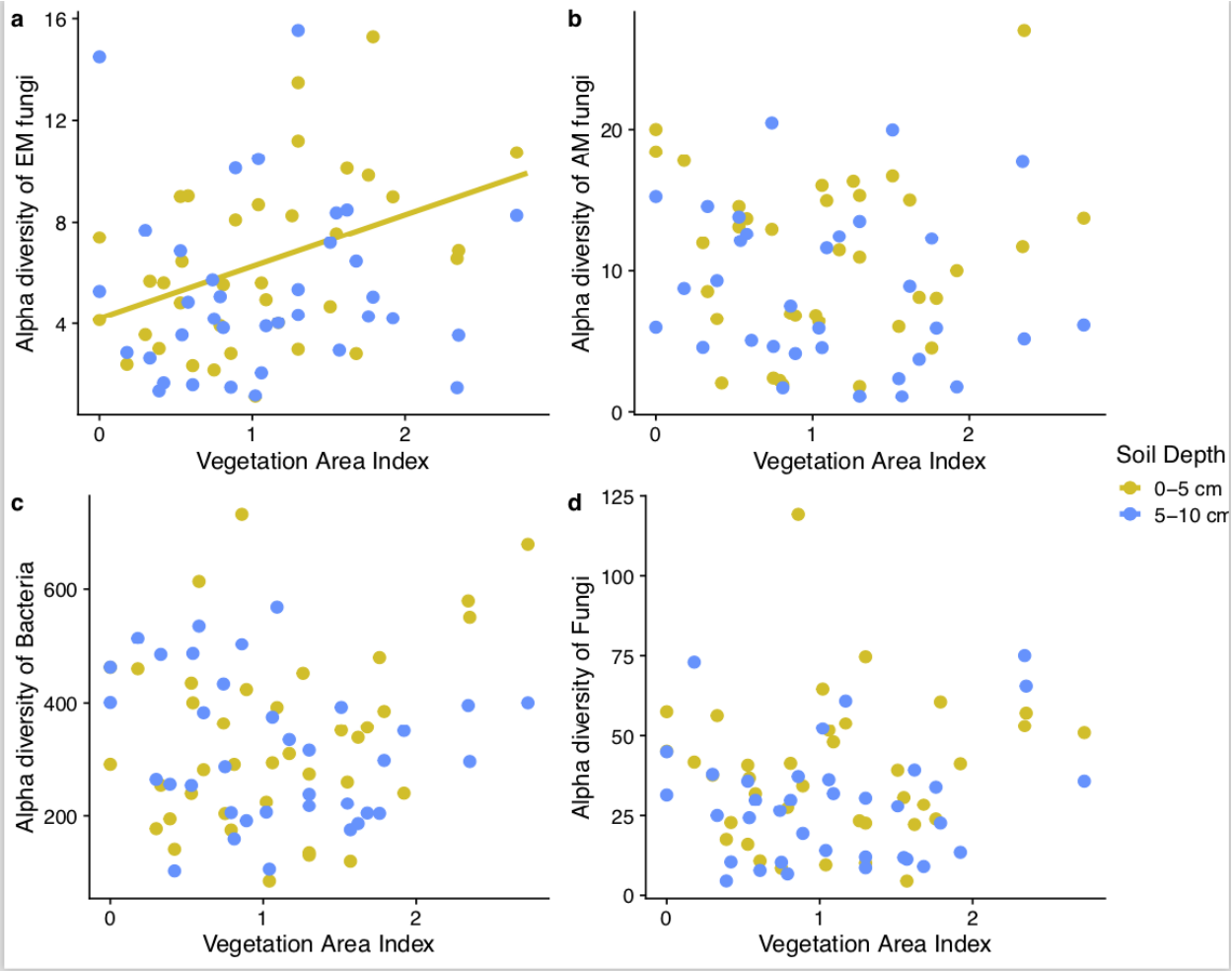

Figure 3. Relationship between vegetation area index (VAI) and alpha diversity of EM fungi, AM fungi, all bacteria, and all fungi, calculated with the inverse Simpson's index. Points represent measured values of microbial richness at 0-5 cm and 5-10 cm soil depths and VAI of plots in forests across Indiana; solid line represents the marginal effect of VAI independent of the effects of other structural diversity variables, and is plotted only for soil depths where the relationship was significant (α=0.05; Table 2).

Structural diversity and environment linkages to microbial beta diversity

Forest structural diversity predicted several components of microbial community composition (beta diversity; Table 3, Table S2). First, individual structural diversity variables of VAI and VertSD predicted variation in EM beta diversity at both soil depths and the total fungi community from 5-10 cm (Table 3). No other components of microbial community composition were predicted significantly by individual structural diversity variables. Second, structural diversity variables as a group significantly predicted variation in the beta diversity of the bacterial and EM fungal community for both 0-5 and 5-10 cm soil depths, and the total fungal community for the 0-5 cm depth (Table S2). Soil properties were always the strongest set of predictors of microbial beta diversity relative to above-ground diversity predictors with the exception of EM fungal beta diversity (Figure 4). Structural diversity variables were stronger predictors of EM beta diversity for 5-10 cm depth.

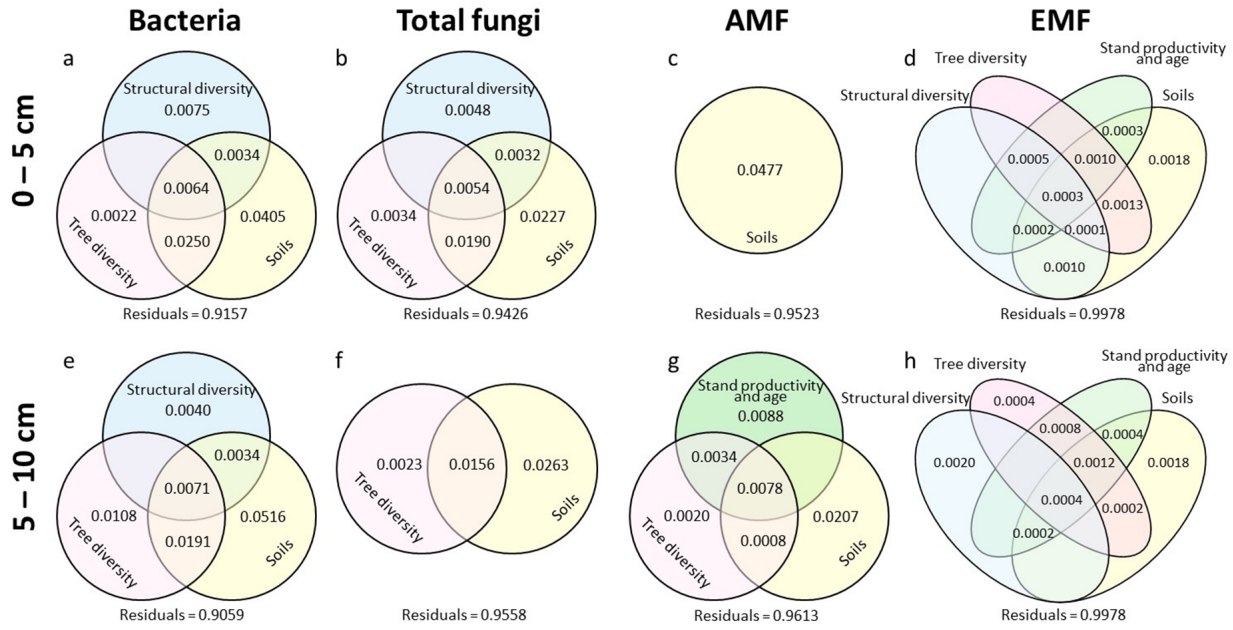

Figure 4. Variance explained by each category of predictors that were indicated significant ($p < 0.05$) in the dbRDA model at 0-5 cm (a-d) and 5-10 cm (e-h) soil depths for bacterial community (ae), total fungal community (bf), AMF community (cg), and EMF community (dh). See Table S2 for model X^2 and p-values for each significant predictor category.

Discussion

We expected that structurally diverse forests would provide habitat, greater resources, or would be associated with successionally older ecosystems, that would promote higher taxonomic diversity of the soil microbial community. Bacterial, fungal, and AM fungal alpha diversity were not associated with structural diversity, but the alpha diversity of EM fungi in particular was positively associated with the density of vegetation within the canopy, which is consistent with our prediction (Dove & Keeton, 2015). A higher density of vegetation layers in the canopy has been associated with more productive stands (Hardiman *et al.*, 2011; Gough *et al.*, 2019), which may influence microbial community composition (Anthony *et al.*, 2022), but vegetation density (VAI) was not strongly correlated with stand productivity in our study system. However, VAI was moderately positively correlated with stand age and stand age was positively correlated with EM alpha diversity in the surface soil (Table 2). This suggests that older stands have canopies with more vertical layers of forest vegetation (Franklin & Van Pelt, 2004; LaRue *et al.*, 2023), and may indicate an uneven age structure of trees that supports a richer community of root-associated EM fungi. We may have only seen this pattern for EM rather than other groups of microbes because the composition of EM fungal communities changes as their host trees age (Reverchon *et al.*, 2012; Birch *et al.*, 2021); uneven-aged stands contain a larger variety of host ages and therefore more opportunities for the establishment of different EM taxa. Notably, although older stands did support greater species richness of EM-associated trees, EM fungal richness was not associated with EM tree species richness, meaning that this pattern is unlikely to be due to concomitant changes in host species richness with stand age (Figure S2). This supports our hypothesis that structural diversity changes with forest ontogeny such that forest managers might be able to link LiDAR-derived information from structurally dense and older forest stands to predict areas with higher EM taxonomic richness in central hardwood forests.

Contrary to our hypotheses that structural diversity would generally lead to greater habitat and resources for microbes, we found that soil bacteria, AM and total fungi were not associated with forest structural diversity. We instead found that soil pH was a strong predictor of alpha diversity among these groups. Bacteria in particular have been shown to be sensitive to acidic soils, whereas not all fungal or mycorrhizal fungal taxa are as sensitive to pH (Porter *et al.*, 1987; Rousk *et al.*, 2009). Alternatively, the species richness and structural diversity of the herbaceous layer may be more important in explaining microbial alpha diversity (Yin *et al.*,

2016; Chen *et al.*, 2021). Future work with terrestrial laser scanning or drones would be better suited to investigate these potential linkages, as measuring the herbaceous structural diversity is not currently possible with aerial LiDAR data due to constraints with data resolution and occlusion by the outer canopy (Li *et al.*, 2021).

The above ground diversity in a forest, whether structural or tree species richness, may be used to predict EM and total fungal community composition. Indeed, beta diversity of the bacterial, EM, and total fungal microbial community (i.e. community composition) in our study was related to forest structural diversity, but structural diversity was a weaker predictor relative to other environmental factors, particularly soil properties. Soil properties such as pH and nutrient content are known to select for taxa that can survive in specific soil conditions (Mitchell *et al.*, 2010; de Vries *et al.*, 2012), but other factors such as plant traits and richness have been shown to impact microbial community diversity just as strongly (Kivlin *et al.*, 2022). However, in our study soil properties and tree diversity were the stronger predictors of community composition over structural diversity. Furthermore, as shown for EM alpha diversity, vegetation density (VAI) was also important for predicting EM beta diversity. Additionally, the vertical heterogeneity (VertSD) predicted EM and diversity of layers in the canopy (VCI) predicted variation in the total fungal community composition. It is possible that these structural profiles of the aboveground forest community do indeed provide habitat or resources (including primary production) that support specific fungal or EM fungal taxa. Further, analysis into the specific taxonomic similarities to more or less structurally diverse forests could pinpoint the mechanisms linking the structural and microbial aspects of forest diversity.

Despite seeing several linkages between structural diversity and the diversity of specific microbial community groups, the relationships overall were weaker and fewer than those observed for other environmental predictors. It is possible that we did not see many aspects of structural diversity or tree species richness be linked to belowground diversity because there is inherently a spatial mismatch between the forest stand level and microbial community scale. It is well established that the magnitude and direction of diversity patterns in ecological relationships can vary with spatial scale (Wiens, 1989; Rollinson *et al.*, 2021). The relative importance of environmental drivers can be variable over space and time and such variation can be hard to capture in their impact on ecological patterns at different scales (Wiens, 1989). The belowground dimensions of diversity change on a smaller spatial and temporal scale than the structural and

379 species composition of forest canopies (Averill *et al.*, 2019, 2021; Kivlin & Hawkes, 2020).
380 Therefore the linkages between above- and belowground components of ecosystems may
381 become decoupled at increasingly large spatial scales (Martiny *et al.*, 2011). For example,
382 microbial richness may be impacted more strongly by soil properties, fine root activity, or
383 individual host species traits on a sub-meter scale rather than stand-level structural or
384 biodiversity (Kivlin & Hawkes, 2016). In our data set, soil properties were measured at the same
385 spatial scale of the microbial community (i.e. within a single soil core) and were therefore more
386 closely matched in sampling spatial scale than the LiDAR or forest inventory data, likely
387 contributing to the relatively higher degree of association between soil conditions and microbial
388 community composition compared with vegetation properties. Future investigations should focus
389 on examining both fine-scale and broad-scale above and below ground diversity data to
390 determine if the strength of their relationships vary across spatial scales.

391 We investigated how forest structural diversity relates to soil microbial diversity within
392 the central hardwoods region, but it is yet unclear how structural diversity may be linked to
393 microbial community composition and richness in other forest types or biomes. Across broad
394 temperature and moisture gradients, abiotic filtering, rather than structural diversity, may limit
395 microbial community richness in forest soils (Nottingham *et al.*, 2018). Soil properties,
396 particularly pH, seem to be a ubiquitous predictor of microbial diversity (van der Linde *et al.*,
397 2018; Davison *et al.*, 2021), and are often connected to plant community composition (Finzi *et*
398 *al.*, 1998; Templer *et al.*, 2005) and changes in temperature and moisture conditions (Seaton *et*
399 *al.*, 2021), but the connections between the drivers of above- and belowground diversity are still
400 largely unexplored (Fei *et al.*, 2022). In order to understand if remote sensing of structural
401 diversity could be used at broad scales to understand microbial diversity patterns, it is necessary
402 to establish the biogeography of these relationships.

403 **Conclusions**

404 Our results indicate that structural diversity at the stand level within the central hardwood
405 region may be less useful for predicting bacterial or fungal taxonomic richness (alpha diversity),
406 but may be useful for linking EM fungal richness to stand vegetation density. Our study also
407 indicates that structural diversity may be able to predict general shifts in community composition
408 of EM and total fungal communities. Restoration research that uses microbial community

409 composition to achieve targeted ecosystem functions might consider the potential of using
410 remote sensing for ecosystem monitoring in relationship to microbial community composition.

411

412 **Acknowledgements:** Funding was provided by NSF DEB #2106103 to SF, EL, GD, #2106096
413 to RP, #2106065 to SK, #2106014 to JP, MM, and NSF DBI #2010724 to AL

414

415 **Author contributions:** AL and EL wrote the first draft of the manuscript. AL, EL, SK, and JE
416 conducted the analyses. AL, EL, JG, RP, NK, and SK collected the data. All authors contributed
417 to writing and editing the manuscript.

418

419 **Data availability:** All data and R code will be made available upon publication and deposited in
420 Zenodo.

421

422 **References**

423 **Anthony MA, Crowther TW, van der Linde S, Suz LM, Bidartondo MI, Cox F, Schaub M,**
424 **Rautio P, Ferretti M, Vesterdal L, *et al.* 2022**. Forest tree growth is linked to mycorrhizal fungal
425 composition and function across Europe. *The ISME journal* **16**: 1327–1336.

426 **Aučina A, Rudawska M, Leski T, Ryliškis D, Pietras M, Riepšas E**. **2011**. Ectomycorrhizal
427 fungal communities on seedlings and conspecific trees of Pinus mugo grown on the coastal
428 dunes of the Curonian Spit in Lithuania. *Mycorrhiza* **21**: 237–245.

429 **Averill C, Bhatnagar JM, Dietze MC, Pearse WD, Kivlin SN**. **2019**. Global imprint of
430 mycorrhizal fungi on whole-plant nutrient economics. *Proceedings of the National Academy of*
431 *Sciences of the United States of America* **116**: 23163–23168.

432 **Averill C, Werbin ZR, Atherton KF, Bhatnagar JM, Dietze MC**. **2021**. Soil microbiome
433 predictability increases with spatial and taxonomic scale. *Nature ecology & evolution* **5**: 747–
434 756.

435 **Birch J, Lutz JA, Turner BL, Karst J**. **2021**. Divergent, age-associated fungal communities of
436 Pinus flexilis and Pinus longaeva. *Forest ecology and management* **494**: 119277.

437 **Brundrett M**. **2004**. Diversity and classification of mycorrhizal associations. *Biological reviews*
438 *of the Cambridge Philosophical Society* **79**: 473–495.

439 **Callahan BJ, McMurdie PJ, Rosen MJ, Han AW, Johnson AJA, Holmes SP**. **2016**. DADA2:
440 High-resolution sample inference from Illumina amplicon data. *Nature methods* **13**: 581–583.

441 **Carson JK, Campbell L, Rooney D, Clipson N, Gleeson DB**. **2009**. Minerals in soil select
442 distinct bacterial communities in their microhabitats. *FEMS microbiology ecology* **67**: 381–388.

443 **Chen K, Hu L, Wang C, Yang W, Zi H, Manuel L**. **2021**. Herbaceous plants influence bacterial
444 communities, while shrubs influence fungal communities in subalpine coniferous forests. *Forest*
445 *ecology and management* **500**: 119656.

Cinelli C, Ferwerda J, Hazlett C, Rudkin A. **2021**. *sensemakr: Sensitivity Analysis Tools for Regression Models*.

Comas LH, Callahan HS, Midford PE. **2014**. Patterns in root traits of woody species hosting arbuscular and ectomycorrhizas: implications for the evolution of belowground strategies. *Ecology and evolution* **4**: 2979–2990.

Davison J, Moora M, Semchenko M, Adenan SB, Ahmed T, Akhmetzhanova AA, Alatalo JM, Al-Quraishy S, Andriyanova E, Anslan S, *et al.* 2021. Temperature and pH define the realised niche space of arbuscular mycorrhizal fungi. *The New phytologist* **231**: 763–776.

Dove NC, Keeton WS. **2015**. Structural Complexity Enhancement increases fungal species richness in northern hardwood forests. *Fungal ecology* **13**: 181–192.

D'Urban Jackson T, Williams GJ, Walker-Springett G, Davies AJ. **2020**. Three-dimensional digital mapping of ecosystems: a new era in spatial ecology. *Proceedings. Biological sciences / The Royal Society* **287**: 20192383.

Fei S, Kivlin SN, Domke GM, Jo I, LaRue EA, Phillips RP. **2022**. Coupling of plant and mycorrhizal fungal diversity: its occurrence, relevance, and possible implications under global change. *The New phytologist*.

Ferlian O, Goldmann K, Eisenhauer N, Tarkka MT, Buscot F, Heintz-Buschart A. **2021**. Distinct effects of host and neighbour tree identity on arbuscular and ectomycorrhizal fungi along a tree diversity gradient. *ISME Communications* **1**: 1–10.

Finzi AC, Canham CD, Van Breemen N. **1998**. Canopy tree soil interactions within temperate forests: Species effects on pH and cations. *Ecological applications: a publication of the Ecological Society of America* **8**: 447–454.

Franklin JF, Van Pelt R. **2004**. Spatial Aspects of Structural Complexity in Old-Growth Forests. *Journal of Forestry* **102**: 22–28.

Gallion J. **2018**. *Classified Forests Report of Continuous Forest Inventory (CFI) Summary of Years 2013-2017*. Indiana DNR.

Gange AC, Brown VK, Sinclair GS. **1993**. Vesicular-Arbuscular Mycorrhizal Fungi : A Determinant of Plant Community Structure in Early Succession. *Functional ecology* **7**: 616–622.

Gelman A. **2008**. Scaling regression inputs by dividing by two standard deviations. *Statistics in medicine* **27**: 2865–2873.

Gough CM, Atkins JW, Fahey RT, Hardiman BS. **2019**. High rates of primary production in structurally complex forests. *Ecology* **100**: e02864.

Gregorich M, Strohmaier S, Dunkler D, Heinze G. **2021**. Regression with Highly Correlated Predictors: Variable Omission Is Not the Solution. *International journal of environmental research and public health* **18**.

Hardiman BS, Bohrer G, Gough CM, Vogel CS, Curtisi PS. **2011**. The role of canopy structural complexity in wood net primary production of a maturing northern deciduous forest. *Ecology* **92**: 1818–1827.

Högberg MN, Högberg P, Myrold DD. **2007**. Is microbial community composition in boreal forest soils determined by pH, C-to-N ratio, the trees, or all three? *Oecologia* **150**: 590–601.

Ishii HT, Tanabe S-I, Hiura T. **2004**. Exploring the Relationships Among Canopy Structure, Stand Productivity, and Biodiversity of Temperate Forest Ecosystems. *Forest Science* **50**: 342–355.

Johnson D, lJdo M, Genney DR, Anderson IC, Alexander lJ. **2005**. How do plants regulate the function, community structure, and diversity of mycorrhizal fungi? *Journal of experimental botany* **56**: 1751–1760.

Jo I, Potter KM, Domke GM, Fei S. **2018**. Dominant forest tree mycorrhizal type mediates understory plant invasions. *Ecology letters* **21**: 217–224.

Kivlin SN, Hawkes CV. **2016**. Temporal and Spatial Variation of Soil Bacteria Richness, Composition, and Function in a Neotropical Rainforest. *PloS one* **11**: e0159131.

Kivlin SN, Hawkes CV. **2020**. Spatial and temporal turnover of soil microbial communities is not linked to function in a primary tropical forest. *Ecology* **101**: e02985.

Kivlin SN, Mann MA, Lynn JS, Kazenel MR, Taylor DL, Rudgers JA. **2022**. Grass species identity shapes communities of root and leaf fungi more than elevation. *ISME Communications* **2**.

Klindworth A, Pruesse E, Schweer T, Peplies J, Quast C, Horn M, Glöckner FO. **2013**. Evaluation of general 16S ribosomal RNA gene PCR primers for classical and next-generation sequencing-based diversity studies. *Nucleic acids research* **41**: e1.

LaRue E, Fahey R, Fuson T, Foster J, Hatala Matthes J, Hardiman B. **2022**. Evaluating the sensitivity of forest structural diversity characterization to LiDAR point density. *Ecosphere* .

LaRue EA, Knott J, Domke G, Chen HYH, Guo Q, Hisano M, Oswalt C, Oswalt S, Kong N, Potter KM, *et al.* 2023. Structural diversity as a reliable and novel predictor for ecosystem productivity. *Frontiers in ecology and the environment*: Accepted.

LaRue EA, Wagner FW, Fei S, Atkins JW, Fahey RT, Gough CM, Hardiman BS. **2020**. Compatibility of Aerial and Terrestrial LiDAR for Quantifying Forest Structural Diversity. *Remote Sensing* **12**: 1407.

Legendre P. **2008**. Studying beta diversity: ecological variation partitioning by multiple regression and canonical analysis. *Journal of Plant Ecology* **1**: 3–8.

Lekberg Y, Vasar M, Bullington LS, Sepp S-K, Antunes PM, Bunn R, Larkin BG, Öpik M. **2018**. More bang for the buck? Can arbuscular mycorrhizal fungal communities be characterized adequately alongside other fungi using general fungal primers? *The New phytologist* **220**: 971–976.

van der Linde S, Suz LM, Orme CDL, Cox F, Andreae H, Asi E, Atkinson B, Benham S, Carroll C, Cools N, *et al.* 2018. Environment and host as large-scale controls of ectomycorrhizal fungi. *Nature* **558**: 243–248.

Li S, Wang T, Hou Z, Gong Y, Feng L, Ge J. **2021**. Harnessing terrestrial laser scanning to predict understory biomass in temperate mixed forests. *Ecological indicators* **121**: 107011.

Loreau M, Naeem S, Inchausti P, Bengtsson J, Grime JP, Hector A, Hooper DU, Huston MA, Raffaelli D, Schmid B, *et al.* 2001. Biodiversity and ecosystem functioning: current knowledge and future challenges. *Science* **294**: 804–808.

Martiny JBH, Eisen JA, Penn K, Allison SD, Horner-Devine MC. **2011**. Drivers of bacterial beta-diversity depend on spatial scale. *Proceedings of the National Academy of Sciences of the United States of America* **108**: 7850–7854.

Matsuo T, Martínez-Ramos M, Bongers F, van der Sande MT, Poorter L. **2021**. Forest structure drives changes in light heterogeneity during tropical secondary forest succession. *The Journal of ecology* **109**: 2871–2884.

McCormack ML, Dickie IA, Eissenstat DM, Fahey TJ, Fernandez CW, Guo D, Helmisaari HS, Hobbie EA, Iversen CM, Jackson RB, *et al.* 2015. Redefining fine roots improves understanding of below-ground contributions to terrestrial biosphere processes. *New Phytologist* **207**.

Midgley MG, Phillips RP. **2016**. Resource stoichiometry and the biogeochemical consequences of nitrogen deposition in a mixed deciduous forest. *Ecology* **97**: 3369–3377.

Mitchell RJ, Hester AJ, Campbell CD, Chapman SJ, Cameron CM, Hewison RL, Potts JM. **2010**. Is vegetation composition or soil chemistry the best predictor of the soil microbial community? *Plant and soil* **333**: 417–430.

Morris EK, Caruso T, Buscot F, Fischer M, Hancock C, Maier TS, Meiners T, Müller C, Obermaier E, Prati D, *et al.* 2014. Choosing and using diversity indices: insights for ecological applications from the German Biodiversity Exploratories. *Ecology and evolution* **4**: 3514–3524.

Nottingham AT, Fierer N, Turner BL, Whitaker J, Ostle NJ, McNamara NP, Bardgett RD, Leff JW, Salinas N, Silman MR, *et al.* 2018. Microbes follow Humboldt: temperature drives plant and soil microbial diversity patterns from the Amazon to the Andes. *Ecology* **99**: 2455–2466.

Oksanen J, Simpson GL, Guillaume Blanchet F, Kindt R, Legendre P, Minchin PR, O'Hara RB, Solymos P, Stevens MHH, Szoecs E, *et al.* 2022. *vegan: Community Ecology Package*.

Opik M, Vanatoa A, Vanatoa E, Moora M, Davison J, Kalwij JM, Reier U, Zobel M. **2010**. The online database MaarjAM reveals global and ecosystemic distribution patterns in arbuscular mycorrhizal fungi (Glomeromycota). *The New phytologist* **188**: 223–241.

Pold G, DeAngelis KM. **2013**. Up against the wall: The effects of climate warming on soil microbial diversity and the potential for feedbacks to the carbon cycle. *Diversity* **5**: 409–425.

Põlme S, Abarenkov K, Henrik Nilsson R, Lindahl BD, Clemmensen KE, Kauserud H, Nguyen N, Kjøller R, Bates ST, Baldrian P, *et al.* 2020. FungalTraits: a user-friendly traits database of fungi and fungus-like stramenopiles. *Fungal diversity* **105**: 1–16.

Porter WM, Robson AD, Abbott LK. **1987**. Field Survey of the Distribution of Vesicular-Arbuscular Mycorrhizal Fungi in Relation to Soil pH. *The Journal of applied ecology* **24**: 659–662.

Reverchon F, Ortega-Larrocea M del P, Bonilla-Rosso G, Pérez-Moreno J. **2012**. Structure

and species composition of ectomycorrhizal fungal communities colonizing seedlings and adult trees of Pinus montezumae in Mexican neotropical forests. *FEMS microbiology ecology* **80**: 479–487.

Rollinson CR, Finley AO, Alexander MR, Banerjee S, Dixon Hamil K-A, Koenig LE, Locke DH, DeMarche ML, Tingley MW, Wheeler K, *et al.* 2021. Working across space and time: nonstationarity in ecological research and application. *Frontiers in ecology and the environment* **19**: 66–72.

Rousk J, Brookes PC, Bååth E. **2009**. Contrasting soil pH effects on fungal and bacterial growth suggest functional redundancy in carbon mineralization. *Applied and environmental microbiology* **75**: 1589–1596.

Roussel J-R, Auty D. **2022**. Airborne LiDAR Data Manipulation and Visualization for Forestry Applications.

Roussel J-R, Auty D, Coops NC, Tompalski P, Goodbody TRH, Meador AS, Bourdon J-F, de Boissieu F, Achim A. **2020**. lidR_ An R package for analysis of Airborne Laser Scanning (ALS) data. *Remote sensing of environment* **251**.

Seaton FM, Reinsch S, Goodall T, White N, Jones DL, Griffiths RI, Creer S, Smith A, Emmett BA, Robinson DA. **2021**. Long-Term Drought and Warming Alter Soil Bacterial and Fungal Communities in an Upland Heathland. *Ecosystems* .

Soares M, Rousk J. **2019**. Microbial growth and carbon use efficiency in soil: Links to fungal-bacterial dominance, SOC-quality and stoichiometry. *Soil biology & biochemistry* **131**: 195–205.

Tabachnick BG, Fidell LS. **2013**. *Using Multivariate Statistics*. Pearson.

Taboada Á, Tárrega R, Calvo L, Marcos E, Marcos JA, Salgado JM. **2010**. Plant and carabid beetle species diversity in relation to forest type and structural heterogeneity. *European journal of forest research* **129**: 31–45.

Taylor DL, Walters WA, Lennon NJ, Bochicchio J, Krohn A, Caporaso JG, Pennanen T. **2016**. Accurate Estimation of Fungal Diversity and Abundance through Improved Lineage-Specific Primers Optimized for Illumina Amplicon Sequencing. *Applied and environmental microbiology* **82**: 7217–7226.

Templer PH, Lovett GM, Weathers KC, Findlay SE, Dawson TE. **2005**. Influence of Tree Species on Forest Nitrogen Retention in the Catskill Mountains, New York, USA. **8**: 1–16.

USGS. **2020**. 2017-2019 Indiana Statewide LiDAR.

Valbuena R, O'Connor B, Zellweger F, Simonson W, Vihervaara P, Maltamo M, Silva CA, Almeida DRA, Danks F, Morsdorf F, *et al.* 2020. Standardizing Ecosystem Morphological Traits from 3D Information Sources. *Trends in ecology & evolution* **35**: 656–667.

de Vries FT, Manning P, Tallowin JRB, Mortimer SR, Pilgrim ES, Harrison KA, Hobbs PJ, Quirk H, Shipley B, Cornelissen JHC, *et al.* 2012. Abiotic drivers and plant traits explain landscape-scale patterns in soil microbial communities. *Ecology letters* **15**: 1230–1239.

Wagg C, Barendregt C, Jansa J, van der Heijden MGA. **2015**. Complementarity in both plant and mycorrhizal fungal communities are not necessarily increased by diversity in the other. *The*

Journal of ecology **103**: 1233–1244.

Wagg C, Jansa J, Schmid B, van der Heijden MGA. **2011**. Belowground biodiversity effects of plant symbionts support aboveground productivity. *Ecology letters* **14**: 1001–1009.

Wagg C, Schlaeppi K, Banerjee S, Kuramae EE, van der Heijden MGA. **2019**. Fungal-bacterial diversity and microbiome complexity predict ecosystem functioning. *Nature communications* **10**: 4841.

White TJ, Bruns T, Lee S, Taylor J, Others. **1990**. Amplification and direct sequencing of fungal ribosomal RNA genes for phylogenetics. *PCR protocols: a guide to methods and applications* **18**: 315–322.

Whitman T, Neurath R, Perera A, Chu-Jacoby I, Ning D, Zhou J, Nico P, Pett-Ridge J, Firestone M. **2018**. Microbial community assembly differs across minerals in a rhizosphere microcosm. *Environmental microbiology* **20**: 4444–4460.

Wiens JA. **1989**. Spatial Scaling in Ecology. *Functional ecology* **3**: 385–397.

Wu H, Xiang W, Ouyang S, Forrester DI, Zhou B, Chen L, Ge T, Lei P, Chen L, Zeng Y, *et al.* 2019. Linkage between tree species richness and soil microbial diversity improves phosphorus bioavailability. *Functional ecology* **33**: 1549–1560.

Yin K, Zhang L, Chen D, Tian Y, Zhang F, Wen M, Yuan C. **2016**. Understory herb layer exerts strong controls on soil microbial communities in subtropical plantations. *Scientific reports* **6**: 27066.

Zak DR, Holmes WE, White DC, Peacock AD. **2003**. Plant diversity, soil microbial communities, and ecosystem function: are there any links? *Ecology*.

Zeng Y, Hao D, Huete A, Dechant B, Berry J, Chen JM, Joiner J, Frankenberg C, Bond-Lamberty B, Ryu Y, *et al.* 2022. Optical vegetation indices for monitoring terrestrial ecosystems globally. *Nature Reviews Earth & Environment*: 1–17.

634

635

636 **Table 1.** The categories of variables predicted to be linked to belowground diversity.

Category	Variable	Unit
Structural diversity	Standard deviation of vegetation height (VertSD)	m
	Vegetation area index (VAI)	m^2/m^3
	Vertical complexity index (VCI)	unitless
Tree diversity	Tree species richness	Species number
	AM dominance	Proportion
	AM tree richness	Species number
	EM tree richness	Species number
Stand productivity and age	Basal area increment (BAI)	m^2/year
	Stand age	Years
Soil properties	Soil pH	Unitless
	C:N ratio	Unitless
	Oxalate extractable iron (Fe_{Ox})	Percent

637

638 **Table 2.** Effects of plant community, productivity, canopy structure, and soil properties on the
639 alpha diversity of soil microbial communities calculated with the inverse Simpson's index.
640 Linear coefficients (β) indicate the strength and direction of the effects of model parameters and
641 are standardized within models to allow for comparison. Partial R^2 and p values are reported only
642 for trends significant at $\alpha = 0.05$.

643

644

645

	0-5 cm				5-10 cm			
	Bacteria	**Total Fungi**	**AM Fungi**	**EM Fungi**	**Bacteria**	**Total Fungi**	**AM Fungi**	**EM Fungi**
Total tree richness	-	-	-	-	-	-	-	-
AM dominance	-	-	-	-	-	-	-	-
Stand age	-	-	-	β= 0.58 R^2= 0.21 p= 0.017	-	-	-	-
BAI	-	-	-	-	-	β= 0.41 R^2= 0.29 p= 0.004	-	-
VertSD	-	-	-	-	-	-	-	-
VAI	-	-	-	β= 0.41 R^2= 0.19 p= 0.023	-	-	-	-
VCI	-	-	-	-	-	-	-	-
C:N	-	-	-	-	-	-	-	-
pH	β= 0.62 R^2= 0.37 p< 0.001	-	β= 0.43 R^2= 0.18 p= 0.029	-	β= 0.63 R^2= 0.25 p= 0.008	β= 0.32 R^2= 0.16 p= 0.042	β= 0.61 R^2= 0.19 p= 0.032	-
Fe_{Ox} (percent)	-	-	-	-	-	-	-	-
N_{plots}	38	37	35	36	36	36	33	36

646

647

648 **Table 3.** Significant predictors of microbial community composition (beta diversity) explained
649 by structural diversity and environmental variables in a distance-based redundancy analysis. X^2

650 and p values are reported only for a predictor category that explains significant variation in the
651 community composition at $\alpha = 0.05$.

	0-5 cm				5-10 cm			
	Bacteria	**Total Fungi**	**AM Fungi**	**EM Fungi**	**Bacteria**	**Total Fungi**	**AM Fungi**	**EM Fungi**
Total tree richness	-	-	-	X^2:49.4 p<0.001	-	-	-	X^2:56.6 p<0.001
AM dominance	X^2:12.1 p<0.001	X^2:15.5 p<0.001	-	X^2:29.5 p<0.001	X^2:17.2 p<0.001	X^2:14.7 p<0.001	X^2:22.7 p<0.001	-
Stand age	-	-	-	X^2:13.5 p<0.001	-	-	X^2:12.9 p<0.001	X^2:24.6 p<0.001
BAI	-	-	-	-	-	-	-	X^2:89.5 p<0.001
VertSD	-	-	-	X^2:12.2 p<0.001	-	-	-	X^2:33.2 p<0.001
VAI	-	-	-	X^2:27.4 p<0.001	-	-	-	X^2:37.6 p<0.001
VCI	-	X^2:11.2 p<0.001	-	-	-	-	-	-
C:N	X^2:7.81 p=0.005	X^2:52.0 p<0.001	X^2:14.6 p<0.001	X^2:333 p<0.001	X^2:38.9 p<0.001	X^2:84.2 p<0.001	X^2:76.3 p<0.001	X^2:188 p<0.001
pH	X^2:143 p<0.001	X^2:9.27 p=0.002	X^2:166 p<0.001	X^2:214 p<0.001	X^2:132 p<0.001	X^2:61.3 p<0.001	X^2:309 p<0.001	X^2:81.6 p<0.001
Fe_{Ox} (percent)	-	X^2:9.01 p=0.028	-	X^2:53.8 p<0.001	-	X^2:27.2 p<0.001	-	X^2:155 p<0.001
N_{plots}	36	37	38	36	34	36	36	36

652

653

654

655